Published in final edited form as:
Toxicon. 2012 March 15; 59(4): 472–486. doi:10.1016/j.toxicon.2011.02.020.

Development of a chimeric recombinant disintegrin as a cost-effective anticancer agent with promising translational potential

Radu Minea, **Corey Helchowski**, **Barbara Rubino**, **Kyle Brodmann**, **Stephen Swenson**, and **Francis Markland Jr**
Department of Biochemistry and Molecular Biology and Norris Comprehensive Cancer Center, University of Southern California, Keck School of Medicine, Los Angeles, CA

Abstract

Vicrostatin (VCN) is a chimeric recombinant disintegrin generated in Origami B (DE3) *E. coli* as a genetic fusion between the C-terminal tail of a **vi**perid disintegrin echistatin and **cro**talid disintegrin contortrostatin (CN). The therapeutic modulation of multiple integrin pathways via soluble disintegrins was previously shown by us and others to elicit potent anti-angiogenic and anti-metastatic effects in several animal cancer models. Despite these favorable attributes, these polypeptides are notoriously difficult to produce recombinantly in significant quantity due to their structure which requires the correct pairing of multiple disulfide bonds for biological activity. In this report, we show that VCN can be reliably produced in large amounts (yields in excess of 200mg of active purified disintegrin per liter of bacterial culture) in Origami B (DE3), an *E. coli* expression strain engineered to support the folding of disulfide-rich heterologous proteins directly in its oxidative cytoplasmic compartment. VCN retains the integrin binding specificity of both parental molecules it was derived from, but with a different binding affinity profile. While competing for the same integrin receptors that are preferentially upregulated in the tumor microenvironment, VCN exerts a potent inhibitory effect on endothelial cell (EC) migration and tube formation in a dose-dependent manner, by forcing these cells to undergo significant actin cytoskeleton reorganization when exposed to this agent *in vitro*. Moreover, VCN has a direct effect on breast cancer cells inhibiting their *in vitro* motility. In an effort to address our main goal of developing a clinically relevant delivery method for recombinant disintegrins, VCN was efficiently packaged in liposomes (LVCN) and evaluated *in vivo* in an animal breast cancer model. Our data demonstrate that LVCN is well tolerated, its intravenous administration inducing a significant delay in tumor growth and an increase in animal survival, results that can be partially explained by potent tumor apoptotic effects.

Keywords

snake venom disintegrins; recombinant disintegrins; breast cancer; engineered bacterial system; liposomal delivery of recombinant proteins

Correspondence and reprint requests: Francis S. Markland, Ph.D., Department of Biochemistry and Molecular Biology, University of Southern California, Keck School of Medicine, 1303 N Mission Road, CRL-106, Los Angeles, CA 90033, USA, Tel: +1-323-224-7981 Fax: +1-323-224-7679, markland@usc.edu.

INTRODUCTION

The ability of transformed cells to evade the restrictive environmental control exerted by the normal tissue architecture and grow in an anchorage-independent fashion is one of cancer's hallmarks (Hanahan and Weinberg, 2000). One class of cell-surface receptors known to play a critical role in the process leading to the acquisition of an anchorage-independent phenotype is represented by the integrins (Hood and Cheresh, 2002).

Integrins are heterodimeric receptors that evolved to mediate the complex cell-ECM interactions that regulate the ability of cells to mechanically sense their microenvironment. In the ecology of multicellular organisms, integrins are major contributors to the homeostasis of tissue architecture by keeping epithelial cells in a differentiated, specialized state (Bissell et al., 2003). Conversely, as epithelia transition to malignancy they evade the microenvironmental constraints by both altering their integrin affinity and avidity for ECM proteins (inside-out signaling) and/or shifting their integrin expression (Hood and Cheresh, 2002; Mizejewski, 1999). The precise roles, however, played by different integrin subunits in various aspects of tumor progression and why some integrins appear to be especially supportive of tumor progression (Desgrosellier et al., 2009) are still poorly understood. Despite these limitations, due to their pivotal roles in cancer biology, integrins represent attractive therapeutic targets. For instance, although it doesn't seem to be essential for the formation of vasculature during development (Reynolds et al., 2002), nor during physiological angiogenesis associated with wound healing or tissue repair (Hamano et al., 2003; Serini et al., 2006), the β3 integrin appears to be critically involved in the regulation of pathological angiogenesis (Mahabeleshwar et al., 2008). Similarly, αvβ5 and α5β1 as well as a number of other integrins (notably α2β1, α4β1, and α6β4) have also been shown to play important roles in tumor angiogenesis (Serini et al., 2006; Silva et al., 2008). These observations prompted the exploration of pharmacological blockade of integrins which was eventually demonstrated to significantly reduce tumor angiogenesis in numerous cancer models and led to the development of several drug candidates that are currently in clinical trials (Folkman, 2007; Nemeth et al., 2007).

Disintegrins are among the most potent soluble ligands of integrins representing a class of cysteine-rich polypeptides historically isolated from the venoms of snakes belonging to the *Viperidae* family (Gould et al., 1990). These natural polypeptides (4–16 kDa), first discovered in 1983 (Ouyang and Huang, 1983) and named in 1990 (Gould et al., 1990), hold a significant translational potential as anti-cancer agents based on their anti-angiogenic and anti-metastatic effects demonstrated in various experimental settings (Huang et al., 2001; McLane et al., 2008; Swenson et al., 2004). In the time that has passed since the first disintegrin was identified almost three decades ago (Ouyang and Huang, 1983), over 100 additional disintegrins have been named and studied (McLane et al., 2008). Despite their enormous therapeutic potential, to the best of our knowledge none of these natural products or their recombinant variants has made it yet into human clinical trials. Nonetheless, many of these natural polypeptides continue to be intensely investigated preclinically in various animal models of human disease while they are evaluated for imagistic and therapeutic applications for pathologies as diverse as cancer, cardiovascular thrombotic events, chronic inflammation, asthma, osteopenia etc. (McLane et al., 2008). From earlier attempts to investigate the anti-thrombotic applications of disintegrins, such as echistatin (Shebuski et al., 1990) and kistrin (Barker et al., 1992; Gold et al., 1991), most subsequent preclinical efforts have focused on the anti-angiogenic and anti-metastatic properties of these compounds for anti-cancer applications (Kang et al., 2000; Kim et al., 2003; Marcinkiewicz et al., 2003; Ramos et al., 2008; Swenson et al., 2004). Another promising clinical application of disintegrins is represented by the tumor imagistic potential of these integrin-targeted molecules. To explore this particular application of disintegrins, McQuade et al.

investigated the tumor specificity of radiolabeled bitistatin (which binds to β3 integrins) in a breast carcinoma animal model (McQuade et al., 2004). In this model, bitistatin was radiolabeled with either ^{125}I or a beta-emitting radionuclide, ^{64}Cu, which is an effective positron emission tomography (PET) tracer. Although preliminary, the results from this imagistic study showed that the tumor specificity of radiolabeled bitistatin was similar or better to that of much smaller RGD-containing peptides and the fact that radiolabeled bitistatin accumulated in tumors that do not themselves express the β3 integrin.

The integrin-binding activity of disintegrins depends on the appropriate pairing of several cysteine residues responsible for the disintegrin fold, a mobile 11-amino acid loop protruding from the polypeptide core displaying a tri-peptide recognition motif, usually RGD (Arg-Gly-Asp), that is conserved in many disintegrins (Moiseeva et al., 2008; Saudek et al., 1991). Although these molecules naturally evolved to efficiently bind to the activated platelet-specific integrin αIIbβ3, thus disrupting the process of platelet aggregation (the final step in blood clotting), most purified snake venom disintegrins are rather promiscuous in that they bind to several β1, β3 or β5 integrin members, albeit with different affinities and selectivity (McLane et al., 1998). Two of the most studied native disintegrins are the homodimer contortrostatin (CN) (Trikha et al., 1994b) and the monomer echistatin (McLane et al., 2008). Similar to echistatin, the anti-tumor activity of CN is based on its high affinity interaction with integrins αvβ3, αvβ5, and α5β1 on both cancer and angiogenic endothelial cells (Trikha et al., 1994a; Zhou et al., 1999; Zhou et al., 2000). We have previously shown (Swenson et al., 2004) that a liposomal formulation of CN can delay tumor growth by significantly reducing the microvascular density in an orthotopic animal cancer model. We provided evidence that disintegrins can be safely and effectively administered intravenously by a clinically acceptable delivery method (i.e., liposomal delivery), and that they passively accumulate at the tumor site. Furthermore, when packaged in liposomes, disintegrins did not interact with the components of blood coagulation system (platelets) nor elicit a neutralizing immune response. Here, we provide further evidence that a chimeric disintegrin, vicrostatin (VCN) can be efficiently made recombinantly in Origami B (DE3) *E. coli*. VCN retains the integrin specificity of CN but it engages these receptors with a unique binding affinity. Unlike cyclic RGD peptides, VCN appears to inappropriately elicit a cascade of signaling events rapidly leading to actin stress fibers disassembly in HUVEC plated on complete Matrigel, an effect that may explain the in vitro anti-migratory effects of VCN against endothelial and cancer cells. Finally, we demonstrate here that liposomal formulations of VCN are efficacious *in vivo*, exerting a potent tumor apoptotic effect in a breast carcinoma animal model and significantly prolonging the survival of these animals.

MATERIALS AND METHODS

Controtrostatin purification

Venom of *Agkistrodon contortrix contortrix* was purchased from Miami Serpentarium (Punta Gorda, FL) and CN was purified as previously described (Trikha et al., 1994b).

Cells and reagents

The MDA-MB-435 cells were obtained from Dr. Janet Price (MD Anderson Cancer Center, Houston, TX) and the MDA-MB-231 cells from Dr. Toshiyuki Yoneda (Osaka University, Osaka, Japan). HUVEC were purchased from PromoCell (Heidelberg, Germany) and maintained according to the manufacturer's protocol. The Origami B (DE3) *E. coli* strain and pET32a expression vector carrying the bacterial thioredoxin A gene (*trxA*) were purchased from Novagen (San Diego, CA). The oligonucleotide primers used for rCN and VCN cloning were synthesized by Operon Biotechnologies, Inc. (Huntsville, AL). The 'Endothelial Cell Tube Formation' plates were purchased from BD Biosciences (San Jose,

CA). The tube formation inhibitor Suramin, the actin modifier Cytochalasin D, and the cyclo(Arg-Gly-Asp-DPhe-Val) peptide were purchased from Calbiochem (San Diego, CA). The complete Matrigel was from BD Biosciences (Bedford, MA). The recombinant TEV protease, Calcein AM, and Rhodamine-Phalloidin were purchased from Invitrogen (Carlsbad, CA). A column-based FITC-labeling kit (EZ-Label) and an endotoxin removal kit were purchased from Pierce (Rockford, IL). The DeadEnd™ Fluorometric TUNEL assay kit was from Promega (Madison, WI). The mouse β3 integrin 7E3 antibody was a gift from Dr. Marian Nakata (Centocor, Horsham, PA). Purified soluble αvβ3 and αvβ5 integrins were purchased from Millipore and soluble recombinant α5β1 integrin from R&D Systems (Minneapolis, MN). All other reagents were purchased from Sigma Chemical Co. (St. Louis, MO). Avastin (bevacizumab) was a gift from Dr. Agustin Garcia (Norris Comprehensive Cancer Center, University of Southern California).

Construction of rCN and VCN expression vectors and recombinant production

rCN and VCN were cloned into pET32a vector downstream of TrxA using a BglII/NcoI set of restriction enzymes. The forward primers for both rCN and VCN introduced a unique TEV protease cleavage site, which made possible the removal of thioredoxin during purification. To build the VCN construct, the nucleotides encoding the C-terminal tail of echistatin were added to CN via an elongated reverse primer. The primers used for rCN were: forward – 5′gttccagatctcgagaatctttacttccaaggagacgctcctgcaaatccgtgctgcga3′, and reverse - 5′gttattcgccatggcttaggcatggaagggatttctgggacagccagcaga3′. The primers used for VCN were: forward - 5′gttccagatctcgagaatctttacttccaaggagacgctcctgcaaatccgtgctgcga3′, and reverse - 5′gttattcgccatggcttaagtagctggacccttgtggggatttctgggacagccagcagatatgcc3′. The bacterial transformants were grown and induced as previously described (Minea et al., 2005) then lysed in a microfluidizer (Microfluidics M-110L, Microfluidics, Newton, MA). The operating conditions of the microfluidizer included applied pressures of 14,000–18,000 psi, bacterial slurry flow rates of 300–400 ml per minute and multiple passes of the slurry through the processor. The lysate insoluble cellular debris was removed by centrifugation (40,000×g) and the soluble material containing either Trx-rCN or Trx-VCN collected. The expressed fusion proteins in the collected soluble lysates were then proteolysed by incubation with recombinant TEV protease overnight at room temperature. When proteolysis was complete, the proteolyzed lysates were passed through a 0.22μm filter, diluted 1:100 in ddH_2O, ultrafiltrated through a 50,000 MWCO cartridge (Biomax50, Millipore) and then reconcentrated against a 5,000 MWCO cartridge (Biomax5, Millipore) using a tangential flow ultrafiltration device (Labscale TFF system, Millipore).

Purification of recombinant disintegrins

Purification was accomplished by C18-reverse phase HPLC using the standard elution conditions previously employed for the purification of native CN (Trikha et al., 1994b). The filtrated lysates processed as described above were loaded onto a Vydac C18 column (218TP54, Temecula, CA). A ten-minute rinse (at 5 ml/min) of the column with an aqueous solution containing 0.1%TFA was followed by a linear gradient (0–100%) elution over 150 min in a mobile phase containing 80% acetonitrile and 0.1%TFA. rCN starts eluting in 30% acetonitrile, while VCN elutes in 35% acetonitrile.

Inhibition of platelet aggregation

The inhibition of ADP-induced platelet aggregation by recombinant disintegrins was determined by measuring the light absorption of human platelet-rich plasma (PRP) in a specialized spectrophotometer (Chrono-log 490 optical aggregometer, Chrono-log, Havertown, PA) as previously described (Swenson et al., 2004). The FITC-labeled disintegrins (FITC-CN and FITC-VCN) and the liposomal formulations of VCN (LVCN) were also tested for activity against platelets.

Mass spectrometry (MS) analysis and sequencing by tryptic digestion

The MS analysis (MALDI-TOF and ESI) was initially done by Dr. Kym Faull (University of California at Los Angeles) and the subsequent sequencing by Dr. Ebrahim Zandi (Keck School of Medicine, University of Southern California). For sequencing, the purified recombinant disintegrin was reduced, alkylated and digested with trypsin at 37°C overnight. The resultant digestion peptides were then used in the tandem LC/MS/MS for sequence analysis. The LC consists of a reverse phase C-18 column through which peptides were eluted into the mass spectrometer using the following gradients: 5–60% acetonitrile + 0.1% formic acid over 75 min and 50–90% acetonitrile + 0.1% formic acid over 10 min. Tandem MS/MS spectra was acquired with Xcalibur software on a linear ion trap LTQ instrument. Data was analyzed using Bioworks, the SEQUEST algorithm and Sage-N Sorcerer to determine cross-correlation scores between acquired spectra and NCBI protein FASTA databases or any other databases as needed.

Cell surface binding studies by flow cytometry

HUVEC, MDA-MB-231 or MDA-MB-435 cells were grown to early confluency and starved overnight in serum-free media. The cells were harvested and resuspended in 1ml of serum-free media (5×10^5cells/condition) before being incubated with different treatments or controls for 30 min at 37°C. At the end of the incubation period, the cells were pelleted, washed in ice-cold PBS containing 5% fetal bovine serum and analyzed in a FACSCalibur scanner. All cells were counterstained with propidium iodide to allow gating of necrotic cells.

Integrin binding kinetics by fluorescence polarization (FP)

Differing concentrations of purified soluble functional integrins (i.e., αvβ3, αvβ5 or α5β1) were incubated with a constant amount of FITC-labeled VCN or CN using an established protocol (Park and Raines, 2004). Upon binding to the much larger integrin, the fluorescent tag on either disintegrin tumbles in solution at a slower rate compared to the unbound state resulting in increased levels of polarization. The measured FP value is a weighted average of FP values of the bound and free fluorescent disintegrins and is therefore a direct measure of the bound fraction. The data were analyzed as for standard radioligand binding, and kinetics of binding determined using Scatchard analysis and a non-linear curve fit. The data were generated in a PTI QuantaMaster QM-4SE spectrofluorometer (Photon Technology International, Birmingham, NJ) using the PTI FeliX32 software for data acquisition and Prism v3.02 (GraphPad Software, La Jolla, CA) for data analysis.

Cell viability studies

HUVEC, MDA-MB-231 or MDA-MB-435 cells were plated in complete media on either plastic or Matrigel-coated 24-well plates (5×10^4cells/well) and allowed to adhere. Native CN or VCN were added to the wells at concentrations ranging from 1–1000nM. Cells receiving no treatment or Actinomycin D were used as controls. The number of viable cells for each condition was quantified colorimetrically after 24hr of incubation using the Cell Titer 96 AQueous cell viability kit (Promega, Madison, WI) according to the manufacturer's protocol. The cell viability was further confirmed by TUNEL staining.

Inhibition of cell migration (the colloidal gold migration assay)

The ability of disintegrins to interfere with HUVEC, MDA-MB-231 or MDA-MB-435 cell migration was assessed on glass coverslips homogenously covered with a fine layer of colloidal gold salt. This assay represents a modified form of a previously described cellular migration assay (Albrecht-Buehler, 1977; Bowersox and Sorgente, 1982; Zetter, 1980). The cell migration generates particle-free tracks ('phagokinetic tracks') on a densely particle-

coated migratory substrate that can act as a permanent record of cellular movement. The gold chloride solution was prepared using 0.342g Hydrogen Tetrachloroaurate(III) (Sigma-Aldrich) dissolved in 50ml dH_2O. Clean round glass coverslips 2.2cm diameter (VWR International) were grasped with forceps from the edge and repeatedly dipped into a 1% BSA solution over a period of several minutes. The BSA slowly adhered to the glass and this process allowed for a better and more uniform gold coating. Excess BSA was allowed to drain off the coverslips at an angle after which the slips were dipped once in 100% ethanol. The coverslips were then rapidly dried with a hand held hair dryer at medium settings and then placed into the wells of a 12-well cell culture plate (VWR International) for further coating with gold salt as previously described (Bowersox and Sorgente, 1982; Zetter, 1980). Microscopic visual inspection of the wells was then performed under 100–200x magnification (Olympus CK2 inverted phase contrast microscope, or Zeiss Axioplan-2 optical microscope). A uniform orange brown speckled appearance on a black background covering the surface of the slides was indicative of a successful preparation. The prepared gold coverslips were further covered with a layer of complete Matrigel (overnight at 37°C). Early passages of serum-starved HUVEC, MDA-MB-231 or MDA-MB-435 cells were then seeded on these coverslips (approximately 3000cells/well) in the presence of various treatments and allowed to migrate at 37°C in the presence of 5%CO_2 for up to 48hrs depending on the cell line, after which the cells were fixed in 4% formaldehyde and further imaged. The quantification of cellular migration was done by computer-assisted image analysis in which each pixel corresponding to the 'phagokinetic tracks' was counted digitally using the 'SimplePCI' imaging software (C-Imaging Systems, Cranberry Township, PA). The pixels were counted in 25 randomly selected microscopic fields captured at x200 magnification for each treatment condition and plotted against the controls.

Inhibition of HUVEC tube formation

'Endothelial Tube Formation' plates precoated with Matrigel were used according to the manufacturer's protocol. HUVEC were seeded in triplicate (3×10^4cells/well) in the presence of various concentrations of either native CN or VCN and incubated for 16hr at 37°C in the presence of 5%CO_2. The tube formation inhibitor Suramin was used as a positive control. At the end of incubation period, cells were stained with Calcein AM and imaged by confocal microscopy (LSM 510 Confocal/Titanium Sapphire Laser). The total length of tubes for each condition was quantitated in multiple fields using the Zeiss LSM Image Browser (Carl Zeiss MicroImaging GmbH, Munich, Germany) and averaged from at least three independent experiments.

Disruption of actin cytoskeleton organization

HUVEC grown in complete media were seeded in triplicate in 8-well chamber slides coated with complete Matrigel (4×10^4cells/well) before being incubated with various treatments for 3hr at 37°C in the presence of 5%CO_2. The actin modifier Cytochalasin D (CytoD) was used as a positive control. At the end of the incubation period, the cells were washed, fixed in 4% formaldehyde, permeabilized in 0.1% Triton X-100 in PBS, and then stained with Rhodamine-Phalloidin and counter-stained with Hoechst 33342 before being imaged by confocal microscopy (LSM 510 Confocal/Titanium Sapphire Laser).

Liposomal encapsulation of VCN

This procedure was carried out as previously described (Minea et al., 2005) by Molecular Express, Inc (Los Angeles, CA) a company specializing in liposomal encapsulation of therapeutic proteins and other drugs. Liposomal VCN (LVCN) particles were generated by either probe sonication at 10% power for 3 to 5 min in a Branson Probe Sonifier or homogenized in a microfluidizer (M110L; Microfluidics, Newton, MA). The homogenized material was processed between 10,000 and 18,000 psi while maintaining an elevated

temperature (45–65°C). Samples from each batch were taken during the process and the size distribution of LVCN was determined with an Ultrafine Particle Analyzer (UPA150; Microtrac, North Largo, FL). After processing, the unencapsulated VCN in each batch was removed by ultrafiltration using an Amicon UF membrane of 100,000 MWCO and the LVCN was further sterilized by filtration through a 0.2μM PVDF filter.

In vivo efficacy studies

MDA-MB-231 cells (2.5×10^6 per inoculum) were harvested and resuspended in complete Matrigel before being inoculated into the mammary fat pads of nude mice as previously described (Swenson et al., 2004). The tumors were allowed to grow for 2 weeks or until they became palpable before treatment was initiated. VCN was administered either encapsulated in different liposomal formulations (at the dose-equivalent of 100μg of VCN per injection) or non-encapsulated, as an aqueous solution (100μg VCN). All VCN administrations were made intravenously (via tail vein) twice a week for the duration of each study. Avastin was administered intravenously (via tail vein) at the dose of 400μg per injection (approx. 20μg/gr.) once a week for the duration of the study. Tumor diameters were measured weekly with a caliper in a blind fashion and the tumor volumes calculated using the formula [length (mm) × width $(mm)^2$]/2, where the width and the length were the shortest and longest diameters, respectively (Osborne et al., 1985). The average tumor volume for each study group was plotted as a function of time and type of treatment during the entire course of each study. The animals were handled and euthanized under the strict guidelines of the Institutional Animal Care and Use Committee (IACUC) of the University of Southern California.

TUNEL staining of tumor sections

For tumor apoptosis, the DeadEnd™ Fluorometric TUNEL assay kit (Promega, Madison, WI) was used according to the manufacturer's protocol. After TUNEL staining, the cell nuclei were counterstained with Hoechst 33342. The nuclei from apoptosis 'hotspot' areas were digitally counted (object counting) using the SimplePCI imaging software on random images (at least 10 images per tumor from multiple tumors per group) captured at x250. The % of cell death was plotted using the formula 'number of $TUNEL^+$ nuclei/total number of nuclei x100' for each treatment group.

Statistical analysis

Statistical significance was analyzed in Prism v.3.2 (GraphPad Software, La Jolla, CA) by unpaired t-test followed by F-test to compare variances. The tumor volume distribution and immunohistochemistry data were assessed by analysis of variance (ANOVA) with a significant overall F-test followed by Dunnett's multiple comparison tests of treatment groups relative to control. Two-tailed $P<0.05$ were considered significant.

RESULTS

Recombinant production of VCN

Bacterial expression—The expression of recombinant disintegrins was in Origami B (DE3), a strain uniquely designed to address the shortcomings of disulfide-rich recombinant protein production in wild-type *E. coli* (LaVallie et al., 1993). The pET32a expression vector and the T7 system are designed for robust expression of heterologous proteins fused to the 109 amino acid bacterial thioredoxin A (TrxA) in DE3 lysogens. In wild-type *E. coli*, TrxA normally functions as a major cytoplasmic reductase under tight regulatory control. However, in the Origami strain, the oxidative redox state perpetuated by defective thioredoxin reductase (TrxB) and glutathione reductase (Gor) enzymes 'tricks' this

bacterium into producing compensatory higher amounts of TrxA reductase in an attempt to restore the wild-type redox equilibrium which in turn drives the robust expression of any recombinant protein genetically fused to TrxA. Another advantage of expressing heterologous proteins fused to TrxA is the high solubility of this bacterial protein, the result of which is that TrxA internally chaperones the recombinant protein fused to it thus keeping it in solution and allowing for higher levels of foreign protein accumulation in the cytoplasm (LaVallie et al., 1993).

To explore the recombinant production of disintegrins in Origami B (DE3), we generated a construct based on the native sequence of CN (referred to as rCN) and a chimeric construct, previously designated as rCN+ (Minea et al., 2005), but now referred to as vicrostatin (VCN). The VCN construct was designed by replacing the C-terminal tail of native CN with the tail of another native disintegrin, echistatin (also known as echistatin alpha), a short-length viperid disintegrin (Fig. 1). The rationale for the VCN design was based on the finding that the C-termini of snake venom disintegrins are important structural elements essential for full disintegrin activity. For instance, the co-crystallization of monomeric disintegrin trimestatin with integrin αvβ3 demonstrates that the C-terminus of this disintegrin also engages the receptor, but in a different region than its disintegrin loop (Fujii et al., 2003). In addition, a previous report (Wierzbicka-Patynowski et al., 1999) had demonstrated that the swapping of C-terminal tails between two native disintegrins may actually lead to the generation of novel chimeric molecules capable of recognizing specific integrins with altered binding affinities.

By employing the recombinant system described above, two fusion proteins (Trx-rCN and Trx-VCN) were successfully expressed in the cytoplasm of Origami B (DE3) (Fig. 2). Although the expression of Trx-VCN was robust in Origami B (DE3), by growing these transformants in modified media we have been able to boost the recombinant production level of VCN by at least one order of magnitude to a final expression yield of approximately 200mg of active purified disintegrin per liter of bacterial culture.

A unique tobacco etch virus (TEV) protease cleavage site was engineered upstream of both disintegrin constructs in order to facilitate their subsequent cleavage from TrxA. TEV is a highly selective protease that recognizes with very high specificity the canonical Glu-Asn-Leu-Tyr-Phe-Gln-Gly amino acid sequence (Carrington and Dougherty, 1988) therefore leaving the target recombinant proteins intact. This high specificity makes TEV an ideal molecular tool for processing recombinant proteins expressed as fusions. The released recombinant disintegrins were further processed and purified by reverse phase HPLC using a protocol originally designed for native disintegrins (see Materials and Methods).

Initial evaluation of recombinant disintegrin activity—The two purified recombinant molecules were initially tested for activity against platelets. Presumably, a main function of snake venom disintegrins in nature is to bind with very high affinity to the activated platelet integrin αIIbβ3, thus efficiently inhibiting (McLane et al., 2008) the last step in blood clotting, the aggregation of platelets, a process mediated by platelet integrin αIIbβ3. However, of the two constructs expressed recombinantly, only chimeric VCN retained full activity against activated αIIbβ3 integrin (with an IC_{50} very similar to native CN), whereas the rCN construct showed no activity in the nanomolar range characteristic of snake venom disintegrins (Fig. 2). Apparently, the latter construct, although soluble, had failed to fold correctly in the region where the binding site of the molecule resides (i.e., the 11-amino acid disintegrin loop), whereas the C-terminal graft in VCN appeared to play an unexpected beneficial role. It is noteworthy that, like VCN, rCN was also expressed as a unique monomeric species as demonstrated on reducing and non-reducing gels (data not shown). Its lack of activity against activated platelets suggests that rCN adopted a non-

native disulfide pattern at least in the disintegrin loop region. Although it is unclear why the rCN construct failed to adopt CN's native dimeric conformation in this recombinant system, this was not the result of unsuccessful disulfide bridge formation. Both recombinant constructs have been probed with Ellman's reagent and found to contain no free thiol groups.

Mass spectrometry analysis and sequencing of VCN—Interestingly, the MS analysis (MALDI-TOF and ESI) demonstrated that, unlike native CN, VCN is a monomer (MW=7146.0). The sequence was subsequently confirmed by tryptic MS sequencing. Based on these data, we speculated that although VCN may have folded correctly in the C-terminal half of the molecule where the disintegrin loop resides, hence its ability to function like a fully active disintegrin, it might have adopted a non-native cysteine pairing in the N-terminal half of the molecule when compared to native CN (Moiseeva et al., 2008), which compromised its dimerization (see Fig. 1 for disulfide bond configuration of native CN).

Cell surface binding analysis by flow cytometry—The ability of VCN to mimic the binding behavior of native CN against different cell lines was tested by flow cytometry (Fig. 2). Our results show that FITC-labeled VCN has a similar binding profile to CN against HUVEC, MDA-MB-231 and MDA-MB-435 cells.

Integrin binding kinetics by fluorescence polarization—To further determine the specific binding affinities of both native CN and VCN to purified (αvβ3 and αvβ5) or recombinant (α5β1) functional integrins, we measured these interactions in solution by fluorescence polarization. From this set of experiments, the dissociation constants for both native CN and VCN (Table 1) were further deduced. These data showed that both disintegrins exhibit nearly identical affinities for αvβ3 and a similar affinity for αvβ5. However, the results demonstrated that there is at least an order of magnitude difference in these molecules'Kd values to α5β1 with VCN showing a improved binding affinity for this receptor compared to native CN.

In vitro functional assays with VCN

Cell viability studies—To understand the impact of VCN on cell viability *in vitro*, we tested a range of VCN concentrations (1–1000nM) on HUVEC, MDA-MB-231 and MDA-MB-435 cells seeded on top of Matrigel (see Materials and methods) and compared the results to native CN. Neither disintegrin showed any significant impact on cell viability irrespective of the concentration used or the length of the incubation time. The cell viability data was generated using a MTS-based colorimetric assay and further confirmed by TUNEL staining (data not shown).

Inhibition of cell migration—Similar to native CN, VCN significantly inhibits HUVEC, MDA-MB-231 or MDA-MB-435 cell migration in a dose-dependent manner (Fig. 3). Cell migration on complete Matrigel is an integrin-dependent mechanism and both disintegrins blocked this process when using different cell lines with significantly different integrin profiles. As determined by us and others, the MDA-MB-435 cells express significantly more copies of αvβ3 integrin than HUVEC or MDA-MB-231 cells, with the latter expressing the least amount. All three cells also express both αvβ5 and α5β1 integrins, with MDA-MB-435 expressing relatively lower amounts of αvβ5 integrin.

Inhibition of HUVEC tube formation—As previously reported with native CN (Golubkov et al., 2003), VCN also potently inhibits HUVEC tube formation in a dose-dependent manner (Fig. 4). In this assay, cells were plated on Matrigel, incubated with various concentrations of each disintegrin, allowed to form tubes, and then compared to

either untreated cells or cells treated with a known tube formation inhibitor (Suramin). The cells were stained with Calcein and further visualized by confocal microscopy. Multiple images were captured from at least three independent experiments and the tubes corresponding to each treatment condition were measured digitally by pixel counting using the 'SimplePCI' imaging software. The data was collected by multiple individuals in a blind fashion and the total tube length averaged and plotted for each data set.

Disruption of HUVEC actin cytoskeleton organization—To assess the effect of VCN on cell morphology and actin cytoskeleton organization, HUVEC were allowed to adhere to complete Matrigel before being exposed to various treatments. While VCN does not detach HUVEC plated on Matrigel, our results show that unlike other integrin ligands, including a small cyclic RGD peptide (the cRGDfV) and an anti-integrin β3 monoclonal antibody (7E3), VCN potently collapses the actin cytoskeleton of HUVEC in the nanomolar range (Fig. 5). This effect can be only partially prevented if the cells are preincubated with either the 7E3 antibody or the cyclic RGD peptide cRGDfV before being exposed to VCN (data not shown).

In vivo studies with VCN

Liposomal encapsulation of VCN—Our previous study showed that liposomal CN has the following characteristics in mice: 1.) no immunogenicity, 2.) extended circulatory half-life, and 3.) undetectable non-target effects (Swenson et al., 2004). In the present study, various batches of LVCN were prepared for *in vivo* testing by either sonication or homogenization under different processing conditions (temperature, pressure etc). The encapsulation efficiency for these batches was determined to be 70% or greater, and the average size of homogenized LVCN was 83nm.

Efficacy studies with LVCN *in vivo*—LVCN was previously tested in an MDA-MB-435 animal model (Minea et al., 2005) where we showed that it efficiently delayed tumor growth while exerting a pronounced anti-angiogenic effect. In the current study VCN was further tested in the MDA-MB-231 breast carcinoma model with similar results (Fig. 6). Importantly, in the aggressive MDA-MB-231 model, in addition to the delay in tumor growth, LVCN was a found to also significantly increase the survival of animals with results very similar to those observed with Avastin (all control animals in this model died by the end of week 7). A group that received unencapsulated VCN (at the dose of 100μg per injection administered twice weekly via tail vein injections) was also evaluated in this breast cancer model. Interestingly, although the direct injection of unencapsulated VCN at the above dose seemed to be very well tolerated by the animals for the entire duration of the study, at this dose regimen there was no a significant difference in terms of both tumor growth inhibition and survival between the unencapsulated VCN and the control groups (data not shown). The lack of response by unencapsulated VCN is not surprising since this group received the same amount of disintegrin and under the same dosing schedule as the one who received LVCN (i.e., 100μg twice weekly). Since liposomal VCN has a much longer circulatory half-life than the naked protein (20.4hr for L^{125}I-VCN vs. 0.4hr for ^{125}I-VCN) and a superior tumor accumulation, it is conceivable that the naked VCN group did not receive a therapeutically efficacious dose. Similarly, Cilengitide, a cyclic RGD pentapeptide developed by Merck KGaA, is administered at much higher doses than LVCN due to a shorter circulatory half-life and tumor availability (Mas-Moruno et al., 2011). Studies to determine the efficacious dose and dosing regimen for naked VCN in multiple tumor animal models are currently ongoing in the Markland laboratory.

Evaluation of tumor apoptosis activity of LVCN—The current study was also aimed at evaluating the effect of LVCN on tumor apoptosis in the MDA-MB-231 breast cancer

model. Unlike the above efficacy study, to evaluate the impact of LVCN on tumor cell death, tumors were allowed to become more established (4 weeks from inoculation) before a short course of treatment (6 doses) with either LVCN or Avastin was started. In this experimental setting, a large and significant difference in the amount of cell death (TUNEL staining) was observed between the LVCN and control groups (Fig. 6). The reason we chose to quantitate the effects of these treatments on tumor apoptosis in more established tumors that received only a short course of therapy rather than in tumors harvested at the end of the above-mentioned efficacy study was that in the latter, despite the significant differences observed in both tumor size and survival, the number of apoptosis events did not appear to be significantly different across the groups at the end of 7 weeks of treatment (data not shown). One possible explanation for this observed discrepancy in the amount of cell death between the two studies might be that in the longer efficacy study, after 7 weeks of treatment, both LVCN and Avastin might have had a tumor stabilization/dormancy effect which might have led to gradual decline in the number of apoptosis events in these treated tumors over the course of treatment. We plan to address this hypothesis in the future by looking at the differences in both tumor apoptosis and cell proliferation in treated and control groups during a time course study.

DISCUSSION

As key regulators of cell migration, integrins function as centripetal signaling platforms or functional hubs (Contois et al., 2009) capable of bi-directionally integrating the signaling circuitries elicited by different classes of cell surface receptors (e.g., the semaphorin/plexin/neuropilin, the growth factor/receptor tyrosine kinase and the cell surface protease systems) with the cellular locomotor apparatus (Ivaska and Heino, 2009). The efficient disruption of integrin-mediated interactions between tumorigenic ECM and angiogenic EC in the tumor microenvironment seems to be critical from the therapeutic standpoint since, as recently reported (Baluk et al., 2005), one important downside of the potent VEGF/PDGF blockade is the persistence of the basement membranes of involuted tumor vessels after both EC and pericytes undergo regression. Thus, the vascular ECM left behind provides a scaffold for the rapid repopulation of these ‘tracks’ with new EC once the anti-VEGF/PDGF treatment is discontinued.

The critical involvement of integrins in both angiogenesis (Contois et al., 2009; Mahabeleshwar et al., 2006) and tumor invasion (Hood and Cheresh, 2002) provides the rationale for developing therapeutic antagonists aimed at disrupting these molecularly intertwined processes (Folkman, 2007). Most efforts of the past were focused on anti-integrin agents targeting the RGD-binding alphav members, a subclass of integrins thought to play pivotal roles in the regulation of pathological angiogenesis, which prompted the development of a number of small RGD-mimetics and monoclonal antibodies (Nemeth et al., 2007; Tucker, 2006).

In this study, we show that a chimeric disintegrin, vicrostatin (VCN), derived from a member of a well characterized family of naturally occurring broad-spectrum integrin inhibitors, could be successfully produced recombinantly in large scale in an engineered bacterial system. In a number of *in vitro* functional assays, VCN is shown to retain the anti-migration/anti-invasion properties of the native molecule contortrostatin (CN) it was derived from. Our previous studies with native CN indicate that this disintegrin may behave like a soluble ECM-mimetic, by potently altering the actin cytoskeleton dynamics and inducing the deactivation of key molecular components of focal adhesions in both adherent HUVEC and glioma cells, which in turn results in a net anti-migratory/anti-invasive effect (Schmitmeier et al., 2005). Compared to native CN, VCN also targets integrins αvβ3, αvβ5, and α5β1, while diplaying a higher affinity than CN for integrin α5β1 (an amino acid

sequence alteration purposefully engineered into VCN). Similar to native CN, recombinant VCN collapses the actin cytoskeleton in endothelial cells cultured in a rich tumorigenic matrix (complete Matrigel) uniquely endowed to support both survival and migration. These effects distinguish VCN from other integrin ligands tested in this setting, among which were a small cyclic RGD peptide and an integrin targeting monoclonal antibody. It is important to emphasize that a methylated variant of the cyclic RGD peptide used in our experiments, the cyclo(Arg-Gly-Asp-DPhe-NMeVal) peptide or Cilengitide, displaying an improved specificity for integrins αvβ3 and αvβ5 (Dechantsreiter et al., 1999; Goodman et al., 2002), has already been tested against solid tumors in a number of clinical trials with mixed results (Hariharan et al., 2007; Reardon et al., 2008). By comparing these different integrin ligands, our *in vitro* data seem to suggest that VCN might have additional signaling properties compared to cyclic RGD peptides and integrin-targeting monoclonal antibodies. Additional mechanistic studies are currently underway in our laboratory in an effort to better understand these signaling, and possibly therapeutic, differences between disintegrins and other soluble integrin ligands.

Although VCN retains native CN's ability to bind the activated αIIbβ3 platelet integrin, like CN (Swenson et al., 2004) it does not interact with quiescent platelets, an *in vitro* observation further corroborated by our *in vivo* findings: no side effects were documented following direct intravenous administration of purified VCN up to 1mg (mice) or to 5mg (rats). It is noteworthy that there is an established link between activated platelets and metastasis (Jurasz et al., 2004; Nash et al., 2002) and from the therapeutic standpoint it may be advantageous to use a polypeptide like VCN that also has the potential to address this mechanism of metastasis. As a small polypeptide, VCN is not expected to be immunogenic, and our preliminary animal studies showed that VCN indeed failed to elicit an antibody response following intravenous infusion. Despite these findings, for enhanced passive targeting of the drug to the tumor site, we opted for liposomal delivery. VCN can be efficiently encapsulated into unilamellar liposomes and our findings indicate that the liposomal formulations of VCN have far superior efficacy compared to the naked polypeptide in the *in vivo* model tested. On the other hand, liposomal delivery has a number of other advantages including the ability to achieve a good therapeutic response at lower doses administered less frequently. As a unique broad-spectrum anti-invasive drug, VCN may hold an advantage over other anti-tumor therapeutic modalities in that it may be better suited to address the cell survival loops operating in the avascular tissue in the early steps of angiogenesis and metastasis (Kim et al., 2000a; Kim et al., 2000b). For instance, recent studies have demonstrated that the usage of various anti-VEGF/PDGF strategies is linked to an increased risk of early metastasis in animal cancer models (Ebos et al., 2009; Paez-Ribes et al., 2009). Although the clinical relevance of these preclinical studies is not yet clear (Ellis and Reardon, 2009), these data support the idea that not only is there an imperative need to design novel anti-angiogenic drugs with better anti-invasive properties, but also to test the impact of standard of care anti-angiogenics (such as Avastin) on metastasis and/or postoperative survival when they are administered in combination with anti-invasive modalities.

In summary, we developed a novel chimeric disintegrin VCN that can be easily and cost-effectively produced recombinantly and shows excellent anti-tumor efficacy in the breast carcinoma model discussed in this report. Furthermore, the liposomal formulation of VCN is shown to have a profound tumor apoptotic effect when tested on significantly more established tumors in the same breast cancer model.

Acknowledgments

We thank Drs. William Ernst and Gary Fujii of Molecular Express, Inc. (Los Angeles, CA) for providing LVCN. We also thank Dr. Nickolas Chelyapov (NanoBiophysics Core) for expert help with fluorescence polarization studies, Dr. Ebrahim Zandi (USC Proteomics Core) for sequencing VCN, the Imaging Core of Doheny Eye Institute and the Clinical Reference Laboratory for technical assistance with confocal imaging and the flow cytometry studies.

Grant support - This research was funded by grant support to F.M. (Susan G. Komen, grant# BCTR0707423; Army Ovarian Cancer Research Program, grant# W81XWH-07-1-0298; NIH, grants # 1R41CA121452 and 1R41CA126001), and to S.S. (California Breast Cancer Research Program, grant# 12IB-0153).

Abbreviations

CN	native contortrostatin
cRGDfV	cyclo(Arg-Gly-Asp-DPhe-Val) peptide
CytoD	cytochalasin D
EC	endothelial cells
ECM	extracellular matrix
FITC	fluorescein isothiocyanate
HUVEC	human umbilical vein endothelial cells
IPTG	isopropyl-1-β-D-thio-1-galactopyranoside
LVCN	liposomal vicrostatin
PDGF	platelet-derived growth factor
rCN	recombinant contortrostatin
SDS–PAGE	sodium dodecyl sulfate–polyacrylamide gel electrophoresis
TEV protease	tobacco etch virus protease
TrxA	thioredoxin A
TUNEL	terminal deoxynucleotidyl transferase dUTP nick end labeling
VEGF	vascular endothelial growth factor
VCN	vicrostatin

References

Albrecht-Buehler G. The phagokinetic tracks of 3T3 cells. Cell. 1977; 11:395–404. [PubMed: 329998]

Baluk P, Hashizume H, McDonald DM. Cellular abnormalities of blood vessels as targets in cancer. Curr Opin Genet Dev. 2005; 15:102–111. [PubMed: 15661540]

Barker PL, Bullens S, Bunting S, Burdick DJ, Chan KS, Deisher T, Eigenbrot C, Gadek TR, Gantzos R, Lipari MT, et al. Cyclic RGD peptide analogues as antiplatelet antithrombotics. J Med Chem. 1992; 35:2040–2048. [PubMed: 1597855]

Bissell MJ, Rizki A, Mian IS. Tissue architecture: the ultimate regulator of breast epithelial function. Curr Opin Cell Biol. 2003; 15:753–762. [PubMed: 14644202]

Bowersox JC, Sorgente N. Chemotaxis of aortic endothelial cells in response to fibronectin. Cancer Res. 1982; 42:2547–2551. [PubMed: 7083147]

Carrington JC, Dougherty WG. A viral cleavage site cassette: identification of amino acid sequences required for tobacco etch virus polyprotein processing. Proc Natl Acad Sci U S A. 1988; 85:3391–3395. [PubMed: 3285343]

Contois L, Akalu A, Brooks PC. Integrins as “functional hubs” in the regulation of pathological angiogenesis. Semin Cancer Biol. 2009

Dechantsreiter MA, Planker E, Matha B, Lohof E, Holzemann G, Jonczyk A, Goodman SL, Kessler H. N-Methylated cyclic RGD peptides as highly active and selective alpha(V)beta(3) integrin antagonists. J Med Chem. 1999; 42:3033–3040. [PubMed: 10447947]

Desgrosellier JS, Barnes LA, Shields DJ, Huang M, Lau SK, Prevost N, Tarin D, Shattil SJ, Cheresh DA. An integrin alpha(v)beta(3)-c-Src oncogenic unit promotes anchorage-independence and tumor progression. Nat Med. 2009

Ebos JM, Lee CR, Cruz-Munoz W, Bjarnason GA, Christensen JG, Kerbel RS. Accelerated metastasis after short-term treatment with a potent inhibitor of tumor angiogenesis. Cancer Cell. 2009; 15:232–239. [PubMed: 19249681]

Ellis LM, Reardon DA. Cancer: The nuances of therapy. Nature. 2009; 458:290–292. [PubMed: 19295595]

Folkman J. Angiogenesis: an organizing principle for drug discovery? Nat Rev Drug Discov. 2007; 6:273–286. [PubMed: 17396134]

Fujii Y, Okuda D, Fujimoto Z, Horii K, Morita T, Mizuno H. Crystal structure of trimestatin, a disintegrin containing a cell adhesion recognition motif RGD. J Mol Biol. 2003; 332:1115–1122. [PubMed: 14499613]

Gold HK, Yasuda T, Jang IK, Guerrero JL, Fallon JT, Leinbach RC, Collen D. Animal models for arterial thrombolysis and prevention of reocclusion. Erythrocyte-rich versus platelet-rich thrombus. Circulation. 1991; 83:IV26–40. [PubMed: 2040069]

Golubkov V, Hawes D, Markland FS. Anti-angiogenic activity of contortrostatin, a disintegrin from Agkistrodon contortrix contortrix snake venom. Angiogenesis. 2003; 6:213–224. [PubMed: 15041797]

Goodman SL, Holzemann G, Sulyok GA, Kessler H. Nanomolar small molecule inhibitors for alphav(beta)6, alphav(beta)5, and alphav(beta)3 integrins. J Med Chem. 2002; 45:1045–1051. [PubMed: 11855984]

Gould RJ, Polokoff MA, Friedman PA, Huang TF, Holt JC, Cook JJ, Niewiarowski S. Disintegrins: a family of integrin inhibitory proteins from viper venoms. Proc Soc Exp Biol Med. 1990; 195:168–171. [PubMed: 2236100]

Hamano Y, Zeisberg M, Sugimoto H, Lively JC, Maeshima Y, Yang C, Hynes RO, Werb Z, Sudhakar A, Kalluri R. Physiological levels of tumstatin, a fragment of collagen IV alpha3 chain, are generated by MMP-9 proteolysis and suppress angiogenesis via alphaV beta3 integrin. Cancer Cell. 2003; 3:589–601. [PubMed: 12842087]

Hanahan D, Weinberg RA. The hallmarks of cancer. Cell. 2000; 100:57–70. [PubMed: 10647931]

Hariharan S, Gustafson D, Holden S, McConkey D, Davis D, Morrow M, Basche M, Gore L, Zang C, O’Bryant CL, Baron A, Gallemann D, Colevas D, Eckhardt SG. Assessment of the biological and pharmacological effects of the alpha nu beta3 and alpha nu beta5 integrin receptor antagonist, cilengitide (EMD 121974), in patients with advanced solid tumors. Ann Oncol. 2007; 18:1400–1407. [PubMed: 17693653]

Hood JD, Cheresh DA. Role of integrins in cell invasion and migration. Nat Rev Cancer. 2002; 2:91–100. [PubMed: 12635172]

Huang TF, Yeh CH, Wu WB. Viper venom components affecting angiogenesis. Haemostasis. 2001; 31:192–206. [PubMed: 11910185]

Ivaska J, Heino J. Interplay between cell adhesion and growth factor receptors: from the plasma membrane to the endosomes. Cell Tissue Res. 2009

Jurasz P, Alonso-Escolano D, Radomski MW. Platelet--cancer interactions: mechanisms and pharmacology of tumour cell-induced platelet aggregation. Br J Pharmacol. 2004; 143:819–826. [PubMed: 15492016]

Kang IC, Kim DS, Jang Y, Chung KH. Suppressive mechanism of salmosin, a novel disintegrin in B16 melanoma cell metastasis. Biochem Biophys Res Commun. 2000; 275:169–173. [PubMed: 10944460]

Kim S, Bell K, Mousa SA, Varner JA. Regulation of angiogenesis in vivo by ligation of integrin alpha5beta1 with the central cell-binding domain of fibronectin. Am J Pathol. 2000a; 156:1345–1362. [PubMed: 10751360]

Kim S, Harris M, Varner JA. Regulation of integrin alpha vbeta 3-mediated endothelial cell migration and angiogenesis by integrin alpha5beta1 and protein kinase A. J Biol Chem. 2000b; 275:33920–33928. [PubMed: 10944524]

Kim SI, Kim KS, Kim HS, Kim DS, Jang Y, Chung KH, Park YS. Inhibitory effect of the salmosin gene transferred by cationic liposomes on the progression of B16BL6 tumors. Cancer research. 2003; 63:6458–6462. [PubMed: 14559837]

LaVallie ER, DiBlasio EA, Kovacic S, Grant KL, Schendel PF, McCoy JM. A thioredoxin gene fusion expression system that circumvents inclusion body formation in the E. coli cytoplasm. Biotechnology (N Y). 1993; 11:187–193. [PubMed: 7763371]

Mahabeleshwar GH, Chen J, Feng W, Somanath PR, Razorenova OV, Byzova TV. Integrin affinity modulation in angiogenesis. Cell Cycle. 2008; 7:335–347. [PubMed: 18287811]

Mahabeleshwar GH, Feng W, Phillips DR, Byzova TV. Integrin signaling is critical for pathological angiogenesis. J Exp Med. 2006; 203:2495–2507. [PubMed: 17030947]

Marcinkiewicz C, Weinreb PH, Calvete JJ, Kisiel DG, Mousa SA, Tuszynski GP, Lobb RR. Obtustatin: a potent selective inhibitor of alpha1beta1 integrin in vitro and angiogenesis in vivo. Cancer Res. 2003; 63:2020–2023. [PubMed: 12727812]

Mas-Moruno C, Rechenmacher F, Kessler H. Cilengitide: the First Anti-Angiogenic Small Molecule Drug Candidate Design, Synthesis and Clinical Evaluation. Anticancer Agents Med Chem. 2011

McLane MA, Joerger T, Mahmoud A. Disintegrins in health and disease. Front Biosci. 2008; 13:6617–6637. [PubMed: 18508683]

McLane MA, Marcinkiewicz C, Vijay-Kumar S, Wierzbicka-Patynowski I, Niewiarowski S. Viper venom disintegrins and related molecules. Proc Soc Exp Biol Med. 1998; 219:109–119. [PubMed: 9790167]

McQuade P, Knight LC, Welch MJ. Evaluation of 64Cu- and 125I-radiolabeled bitistatin as potential agents for targeting alpha v beta 3 integrins in tumor angiogenesis. Bioconjug Chem. 2004; 15:988–996. [PubMed: 15366951]

Minea R, Swenson S, Costa F, Chen TC, Markland FS. Development of a novel recombinant disintegrin, contortrostatin, as an effective anti-tumor and anti-angiogenic agent. Pathophysiol Haemost Thromb. 2005; 34:177–183. [PubMed: 16707923]

Mizejewski GJ. Role of integrins in cancer: survey of expression patterns. Proc Soc Exp Biol Med. 1999; 222:124–138. [PubMed: 10564536]

Moiseeva N, Bau R, Swenson SD, Markland FS Jr, Choe JY, Liu ZJ, Allaire M. Structure of acostatin, a dimeric disintegrin from Southern copperhead (Agkistrodon contortrix contortrix), at 1.7 A resolution. Acta Crystallogr D Biol Crystallogr. 2008; 64:466–470. [PubMed: 18391413]

Nash GF, Turner LF, Scully MF, Kakkar AK. Platelets and cancer. Lancet Oncol. 2002; 3:425–430. [PubMed: 12142172]

Nemeth JA, Nakada MT, Trikha M, Lang Z, Gordon MS, Jayson GC, Corringham R, Prabhakar U, Davis HM, Beckman RA. Alpha-v integrins as therapeutic targets in oncology. Cancer Invest. 2007; 25:632–646. [PubMed: 18027153]

Osborne CK, Hobbs K, Clark GM. Effect of Estrogens and Antiestrogens on Growth of Human Breast Cancer Cells in Athymic Nude Mice. Cancer Res. 1985; 45:584–590. [PubMed: 3967234]

Ouyang C, Huang TF. Potent Platelet Aggregation Inhibitor from Trimeresurus gramineus Snake Venom. Biochim Biophys Acta. 1983; 757:332–341. [PubMed: 6849980]

Paez-Ribes M, Allen E, Hudock J, Takeda T, Okuyama H, Vinals F, Inoue M, Bergers G, Hanahan D, Casanovas O. Antiangiogenic therapy elicits malignant progression of tumors to increased local invasion and distant metastasis. Cancer Cell. 2009; 15:220–231. [PubMed: 19249680]

Park SH, Raines RT. Fluorescence polarization assay to quantify protein-protein interactions. Methods Mol Biol. 2004; 261:161–166. [PubMed: 15064456]

Ramos OH, Kauskot A, Cominetti MR, Bechyne I, Salla Pontes CL, Chareyre F, Manent J, Vassy R, Giovannini M, Legrand C, Selistre-de-Araujo HS, Crepin M, Bonnefoy A. A novel alpha(v)beta (3)-blocking disintegrin containing the RGD motive, DisBa-01, inhibits bFGF-induced

angiogenesis and melanoma metastasis. Clinical & experimental metastasis. 2008; 25:53–64. [PubMed: 17952617]

Reardon DA, Nabors LB, Stupp R, Mikkelsen T. Cilengitide: an integrin-targeting arginine-glycine-aspartic acid peptide with promising activity for glioblastoma multiforme. Expert Opin Investig Drugs. 2008; 17:1225–1235.

Reynolds LE, Wyder L, Lively JC, Taverna D, Robinson SD, Huang X, Sheppard D, Hynes RO, Hodivala-Dilke KM. Enhanced pathological angiogenesis in mice lacking beta3 integrin or beta3 and beta5 integrins. Nature Medicine. 2002; 8:27–34.

Saudek V, Atkinson RA, Pelton JT. Three-dimensional structure of echistatin, the smallest active RGD protein. Biochemistry. 1991; 30:7369–7372. [PubMed: 1854743]

Schmitmeier S, Markland FS, Schonthal AH, Chen TC. Potent mimicry of fibronectin-induced intracellular signaling in glioma cells by the homodimeric snake venom disintegrin contortrostatin. Neurosurgery. 2005; 57:141–153. discussion 141–153. [PubMed: 15987550]

Serini G, Valdembri D, Bussolino F. Integrins and angiogenesis: a sticky business. Exp Cell Res. 2006; 312:651–658. [PubMed: 16325811]

Shebuski RJ, Ramjit DR, Sitko GR, Lumma PK, Garsky VM. Prevention of canine coronary artery thrombosis with echistatin, a potent inhibitor of platelet aggregation from the venom of the viper, Echis carinatus. Thromb Haemost. 1990; 64:576–581. [PubMed: 2084943]

Silva R, D'Amico G, Hodivala-Dilke KM, Reynolds LE. Integrins: the keys to unlocking angiogenesis. Arterioscler Thromb Vasc Biol. 2008; 28:1703–1713. [PubMed: 18658045]

Swenson S, Costa F, Minea R, Sherwin RP, Ernst W, Fujii G, Yang D, Markland FS Jr. Intravenous liposomal delivery of the snake venom disintegrin contortrostatin limits breast cancer progression. Mol Cancer Ther. 2004; 3:499–511. [PubMed: 15078994]

Trikha M, De Clerck YA, Markland FS. Contortrostatin, a snake venom disintegrin, inhibits beta 1 integrin-mediated human metastatic melanoma cell adhesion and blocks experimental metastasis. Cancer Res. 1994a; 54:4993–4998. [PubMed: 7520832]

Trikha M, Rote WE, Manley PJ, Lucchesi BR, Markland FS. Purification and characterization of platelet aggregation inhibitors from snake venoms. Thromb Res. 1994b; 73:39–52. [PubMed: 8178312]

Tucker GC. Integrins: molecular targets in cancer therapy. Curr Oncol Rep. 2006; 8:96–103. [PubMed: 16507218]

Wierzbicka-Patynowski I, Niewiarowski S, Marcinkiewicz C, Calvete JJ, Marcinkiewicz MM, McLane MA. Structural requirements of echistatin for the recognition of alpha(v)beta(3) and alpha(5)beta(1) integrins. J Biol Chem. 1999; 274:37809–37814. [PubMed: 10608843]

Zetter BR. Migration of capillary endothelial cells is stimulated by tumour-derived factors. Nature. 1980; 285:41–43. [PubMed: 6990271]

Zhou Q, Nakada MT, Arnold C, Markland FS. Contortrostatin, a dimeric disintegrin from *Agkistrodon contortrix contortrix*, inhibits angiogenesis. Angiogenesis. 1999; 3:259–269. [PubMed: 14517425]

Zhou Q, Nakada MT, Brooks PC, Swenson SD, Ritter MR, Argounova S, Arnold C, Markland FS. Contortrostatin, a homodimeric disintegrin, binds to integrin alphavbeta5. Biochem Biophys Res Commun. 2000; 267:350–355. [PubMed: 10623623]

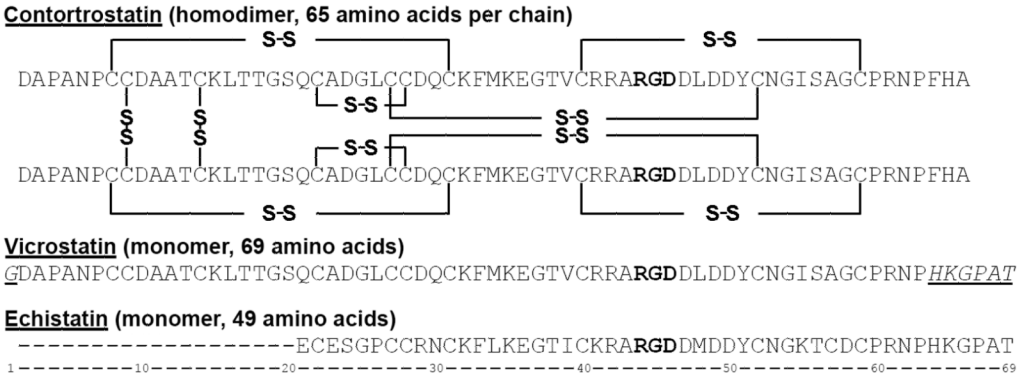

Figure 1. Sequence alignment of contortrostatin (CN), vicrostatin (VCN), and echistatin

VCN is a modified CN sequence that was generated recombinantly by swapping the C-terminal tail of CN with the tail of echistatin. Mass spectrometry and crystallographic data have shown that CN is a dimer with two identical chains oriented in an antiparallel fashion and held together by two interchain disulfide bonds. Unlike native CN, mass spectrometry has confirmed that VCN is a monomer. In the above sequences, the Arg-Gly-Asp tripeptide motif is depicted in bold whereas the non-native amino acids in VCN are both italicized and underlined.

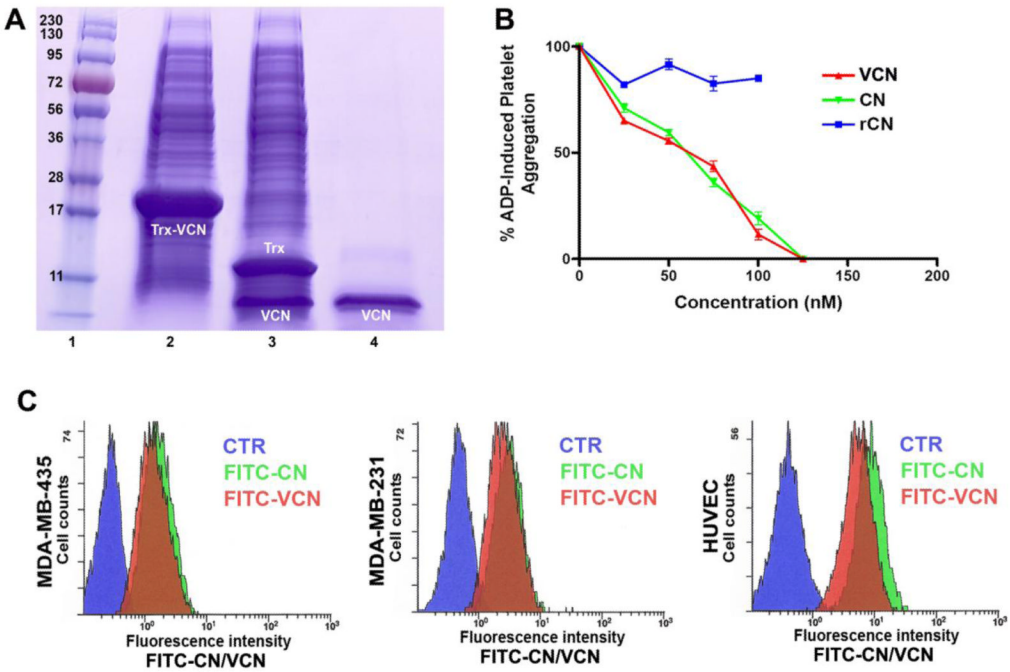

Figure 2. The expression, purification and binding analysis of FITC-labeled disintegrins by flow cytometry

Panel A – Coomassie stained gel showing the migration of Trx-VCN before and after TEV proteolysis (lanes 2 and 3, respectively) versus C18 reverse phase-HPLC purified VCN (lane 4). The same amount (5μl) of cell lysates before and after TEV proteolysis was loaded on a precast gel and Coomassie stained. **Panel B –** VCN and native CN exhibit an almost identical dose-dependent inhibitory effect against ADP-induced platelet aggregation when incubated with human platelet-rich plasma (with a calculated IC_{50} of ~60nM). In contrast, a recombinant construct based on the exact CN sequence (designated rCN), which is also expressed as a soluble polypeptide in Origami B (DE3), shows no inhibitory activity. **Panel C –** Labeled disintegrins (FITC-CN and FITC-VCN) bind in a similar manner to cells displaying different integrin profiles as determined by flow cytometry. MDA-MB-435, MDA-MB-231 or HUVEC were either incubated with FITC-CN (green) or FITC-VCN (red) or probed with an FITC-labeled irrelevant antibody control (blue).

Figure 3(i):

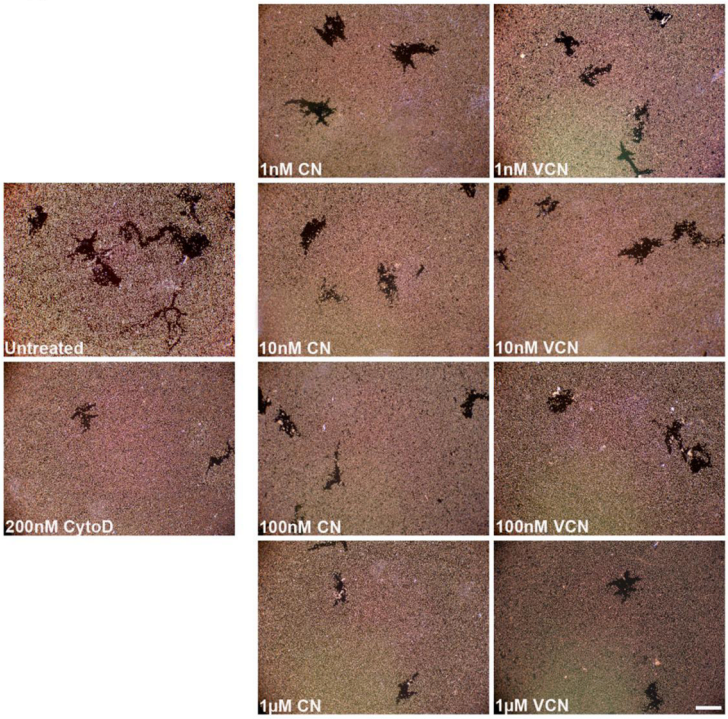

Figure 3(ii):

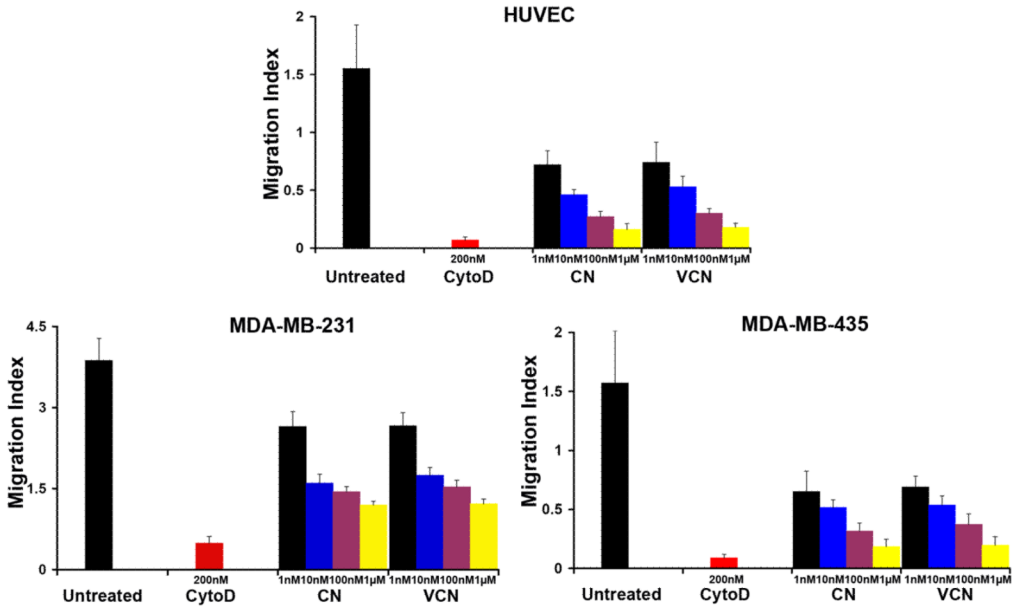

Figure 3. Inhibition of cell migration (the colloidal gold migration assay) by disintegrins

The ability of VCN to disrupt cell migration was assessed on gold coverslips coated with complete Matrigel on which serum-starved HUVEC, MDA-MB-231 or MDA-MB-435 cells were seeded and allowed to adhere before being incubated for up to 48hr with various concentrations of disintegrins (1–1000nM). The fungal metabolite Cytochalasin D, a potent inhibitor of actin polymerization, was used as a positive control at a concentration of 200nM. **(i)** Representative images of ‘phagokinetic tracks’ generated on colloidal gold by

migratory HUVEC exposed to different concentrations of disintegrins (magnification, x200; scale bar, 200μm). **(ii)** The 'phagokinetic tracks' generated by migratory cells with different integrin profiles (HUVEC, MDA-MB-231 or MDA-MB-435) were quantitated digitally ('SimplePCI' imaging software) by counting the total number of pixels corresponding to every track in multiple photomicrographs for each condition. The above plotted data were averaged from multiple independent experiments for each cell line tested.

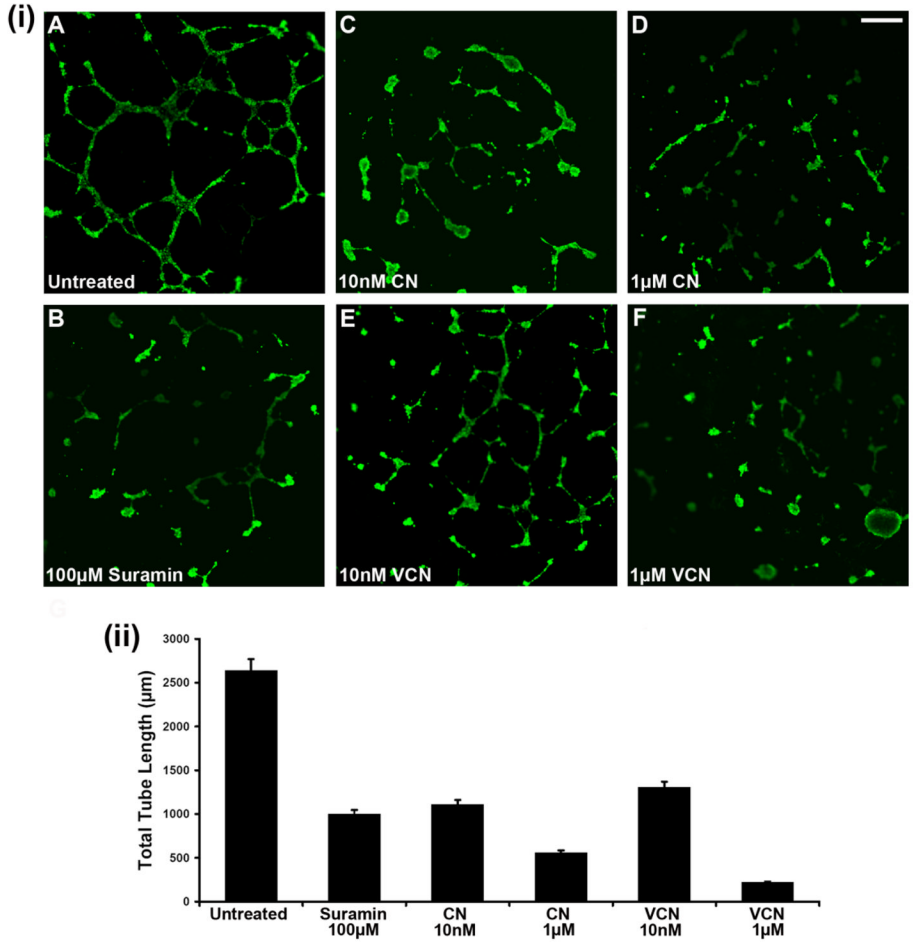

Figure 4. Inhibition of HUVEC tube formation (tubulogenesis) on Matrigel

HUVEC were plated on 'Endothelial Cell Tube Formation' plates (BD Biosciences) and allowed to adhere before being incubated overnight with various concentrations of either CN or VCN (10–1000nM) at 37°C in the presence of 5%CO_2. Suramin, a known tube formation inhibitor, was used as a positive control at a concentration of 100μM. At the end of incubation period, the cells were stained with Calcein AM and imaged by confocal microscopy. **(i)** Representative HUVEC images from three independent experiments (magnification, x25; scale bar, 200μm). **(ii)** The degree of tubulogenesis was assessed on multiple photomicrographs for each condition on which the total length of the tubes was measured and computed in multiple fields using the Zeiss LSM Image Browser (Carl Zeiss MicroImaging GmbH) and then averaged to form each data point. The data presented above was assembled from three independent experiments.

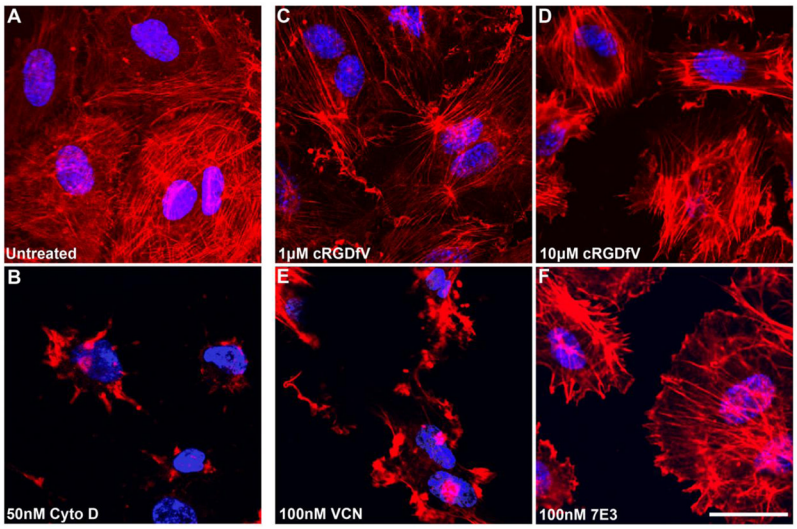

Figure 5. VCN induces massive actin cytoskeleton reorganization in HUVEC seeded on Matrigel

HUVEC were seeded in multiwell chamber slides in serum-free media on complete Matrigel, allowed to adhere, and then treated for 3hr with various concentrations of either a cRGDfV peptide (1 or 10μM), VCN (100nM) or the anti-αvβ3 monoclonal antibody 7E3 (100nM). The actin modifier Cytochalasin D was used as a positive control at a concentration of 50nM. At the end of the incubation period, the cells from all conditions were fixed in 4% formaldehyde, permeabilized in 0.1% Triton X-100, and had their actin cytoskeletons stained with Rhodamine-Phalloidin and nuclei counterstained with Hoechst 33342. Shown above are representative confocal images from multiple experiments taken at the same magnification (x1000; scale bar, 20μm).

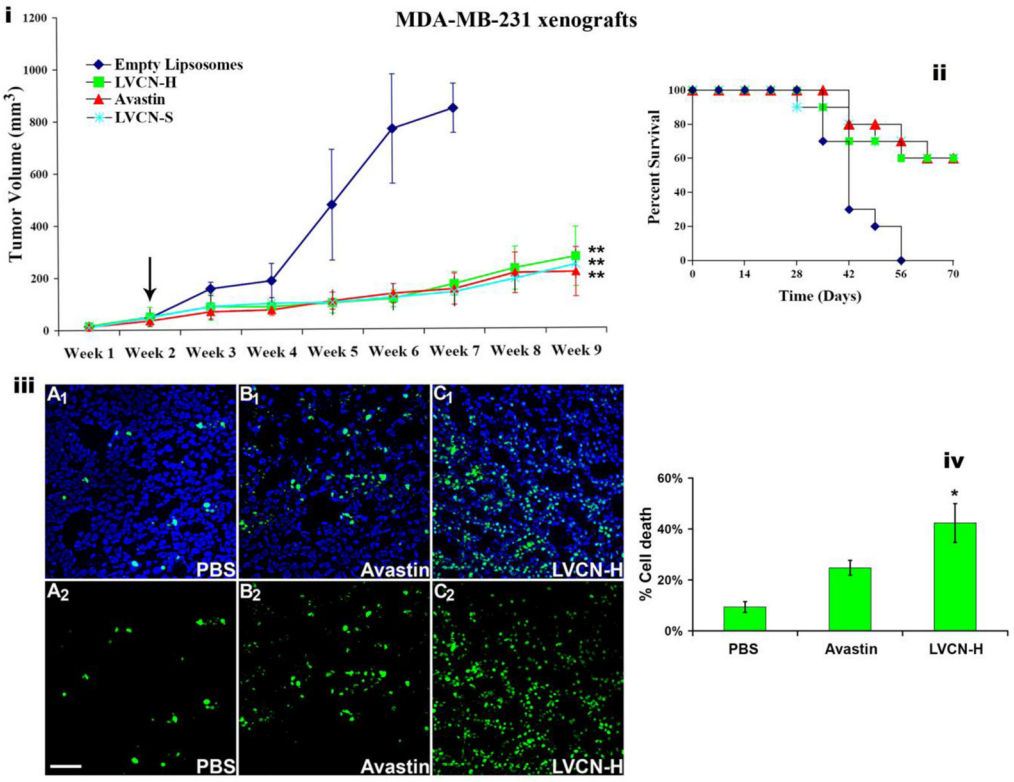

Figure 6. The anti-tumor activity of liposomal VCN (LVCN) in MDA-MB-231 breast carcinoma xenograft model

Nude mice inoculated orthotopically (mammary fat pads; 2.5×10^6 cells) were allowed to grow palpable tumors before treatment was commenced (indicated by the arrow). Two different liposomal formulation of VCN were tested in this study: LVCN-S (prepared by sonication) and LVCN-H (prepared by homogenization). The groups of animals (n=10) were treated intravenously with either LVCN-H or LVCN-S (the dose-equivalent of 100μg of VCN per injection) each administered twice a week, or Avastin (400μg per injection; approx. 20μg/gr) administered once a week. The control group received empty liposomes only. When compared to the control group, a significant delay in tumor growth **(i)** and increased survival **(ii)** was observed in all treated groups. ANOVA was used for statistical analysis followed by Dunnett's multiple comparison tests (** signifies a $P<0.001$). **(iii)** In a different study, designed to assess the ability of VCN to induce tumor apoptosis, MDA-MB-231 xenografts were allowed to grow to a significantly larger volume (4 weeks after inoculation) before the treatments were initiated. These animals received 6 consecutive doses of either LVCN (at the dose-equivalent of 100μg of VCN per injection) or Avastin (400μg per injection) administered intravenously every other day and compared to a control group that received saline only. Tumor cryostat sections from each group were stained with FITC-TUNEL, and counterstained with Hoechst 33342. Representative confocal images from multiple experiments taken at x250 magnification are shown above (scale bar, 100μm; panels A_1-C_1 - TUNEL-Hoechst, panels A_2-C_2 - TUNEL only). **(iv)** The amount of cell death was quantitated as 'number of $TUNEL^+$ nuclei/total number of nuclei x 100' by counting all nuclei in 'hotspot' areas from multiple fields using a computer-assisted approach (the 'SimplePCI' imaging software). The LVCN group shows a significantly increased amount of cell death compared to either Avastin or PBS control. The data was analyzed with ANOVA followed by *post-hoc* tests (* signifies a $P<0.01$).

Table 1
Disintegrin-integrin binding kinetics by fluorescence polarization

The binding kinetics were calculated by measuring the steady state binding of FITC-labeled disintegrins to either purified (αvβ3 and αvβ5) or recombinant (α5β1) functional human integrins. The dissociation constants for interactions of either CN or VCN with soluble integrins were determined by Scatchard analysis using a non-linear curve fit.

Disintegrin	Integrin Kd (+/−SD)		
	αvβ3	α5β1	αvβ5
CN	6.6nM (0.8)	191.3nM(65.2)	19.5nM (5.7)
VCN	7.4nM (0.4)	15.2nM (4.2)	41.2nM (12.3)